The onset of multi-valued solutions of a prescribed mean curvature equation with singular nonlinearity

N. D. BRUBAKER[1] and A. E. LINDSAY[2]

[1] *Department of Mathematical Sciences, University of Delaware, Newark, DE 19716, USA.*
email: brubaker@math.udel.edu
[2] *Department of Mathematics and Maxwell Institute for Mathematical Sciences, Heriot-Watt University, Edinburgh, UK, EH14 4AS.*
email: a.lindsay@hw.ac.uk

(*Received 12 February 2013*)

The existence and multiplicity of solutions to a quasilinear, elliptic partial differential equation (PDE) with singular non-linearity is analyzed. The PDE is a recently derived variant of a canonical model used in the modeling of micro-electromechanical systems (MEMS). It is observed that the bifurcation curve of solutions terminates at single *dead-end* point, beyond which no classical solutions exist. A necessary condition for the existence of solutions is developed, revealing that this dead-end point corresponds to a blow-up in the solution's gradient at a point internal to the domain. By employing a novel asymptotic analysis in terms of two small parameters, an accurate characterization of this dead end point is obtained. An arc length parameterization of the solution curve can be employed to continue solutions beyond the dead-end point, however, all extra solutions are found to be multivalued. This analysis therefore suggests the dead-end is a bifurcation point associated with the onset of multivalued solutions for the system.

Key Words: Prescribed mean curvature, Disappearing solutions, Singular perturbation, MEMS, Singular nonlinearity

1 Introduction and statement of main results

A micro-electromechanical systems (MEMS) capacitor consists of two surfaces held opposite of one another. The lower surface is a rigid inelastic ground plate, while the upper surface is a thin elastic membrane that is held fixed along its boundary and is free to deflect in the presence of a potential difference V (cf. Figure 1). When V is small enough, a stable equilibrium deflection is attained by the membrane; however, if V exceeds a critical value V^*, called the *pull-in* voltage, an equilibrium deflection is no longer attainable and the upper surface will *touchdown* on the lower surface. This loss of a stable equilibrium is called the *pull-in instability* and the mathematical modeling of its onset has been the focus of numerous studies (for a thorough account, see [7, 20] and the references therein). Recently to address the discrepancy between theoretical predictions of V^* and

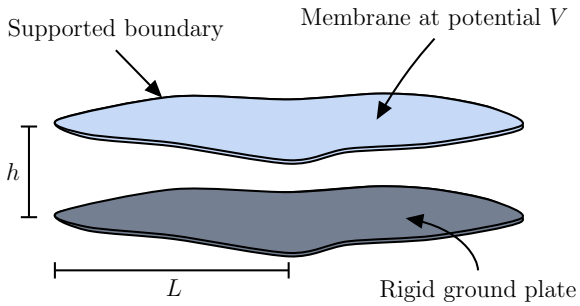

FIGURE 1. Schematic diagram of a MEMS capacitor.

experimental data, the following quasilinear, elliptic partial differential equation (PDE) for the dimensionless equilibrium deflection $z = u(x, y)$ was derived [1, 2]:

$$\operatorname{div} \frac{\nabla u}{\sqrt{1+\varepsilon^2|\nabla u|^2}} = \frac{\lambda}{(1+u)^2} \quad \text{in } \Omega, \tag{1.1 a}$$

$$u = 0 \quad \text{on } \partial\Omega. \tag{1.1 b}$$

Here, ε is the aspect ratio h/L of the device, $\lambda \propto V^2$ is a nonnegative dimensionless parameter quantifying the relative strengths of the elastic and electrostatic forces in the system and Ω is a bounded region in $\mathbb{R}^2$ with boundary $\partial\Omega$. The left-hand side of equation (1.1 *a*) captures the elastic effects of the membrane and comes from minimizing a surface area functional. In particular, equation (1.1 *a*) can be written geometrically as

$$2H/\varepsilon = \frac{\lambda}{(1+u)^2}, \tag{1.2}$$

where H is the mean curvature of the non-parametric surface $(x, y, \varepsilon u(x, y))$ in Ω.

In typical applications, the aspect ratio ε is a small quantity and many MEMS researchers simplify PDE (1.1 *a*) by linearizing the left-hand side, yielding

$$\Delta u = \frac{\lambda}{(1+u)^2} \quad \text{in } \Omega, \qquad u = 0 \quad \text{on } \partial\Omega. \tag{1.3}$$

This reduced problem has been extensively studied and many of its properties are well known (cf. [7, 10, 13, 14, 20]). One of the canonical properties is the existence of a critical value, λ^*, such that for each $\lambda < \lambda^*$, problem (1.3) admits a unique stable solution. At the end of this branch of stable solutions there is a saddle node bifurcation, and no solutions exist for $\lambda > \lambda^*$. When Ω is taken to be the unit ball $B_1(0) = \{\mathbf{x} \in \mathbb{R}^2 : |\mathbf{x}| < 1\}$, the unstable solution branch undergoes infinitely many additional saddle node bifurcations [11], leading to higher multiplicity in the solution set (see Figure 2). However when $\varepsilon \neq 0$, the solution set (λ, u) of problem (1.1) can be markedly different from that of problem (1.3). Specifically, it was numerically observed in [1] that the bifurcation curve $(\lambda(\varepsilon), \|u\|_\infty)$ of problem (1.1) in the unit ball undergoes a finite number of folds before terminating at a single *dead-end* point, denoted $(\lambda_*(\varepsilon), \alpha_*(\varepsilon))$ (see Figure 3). The focus of this paper is to explain and analyze this profound difference between the solution structures of problems (1.1) and (1.3) in the two-dimensional unit ball $B_1(0)$ in the singular limit $\|u\|_\infty \to 1^-$. In particular, we show that as the solution curve approaches

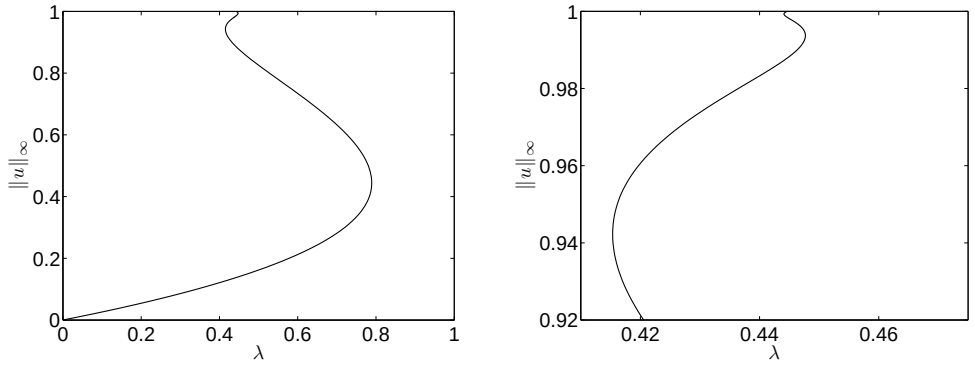

(a) (b) Zoomed

FIGURE 2. (a) Bifurcation diagram of problem (1.3) for Ω equal to the two-dimensional unit ball. (b) A magnified portion of (a) revealing more of the infinite fold structure proved in [11].

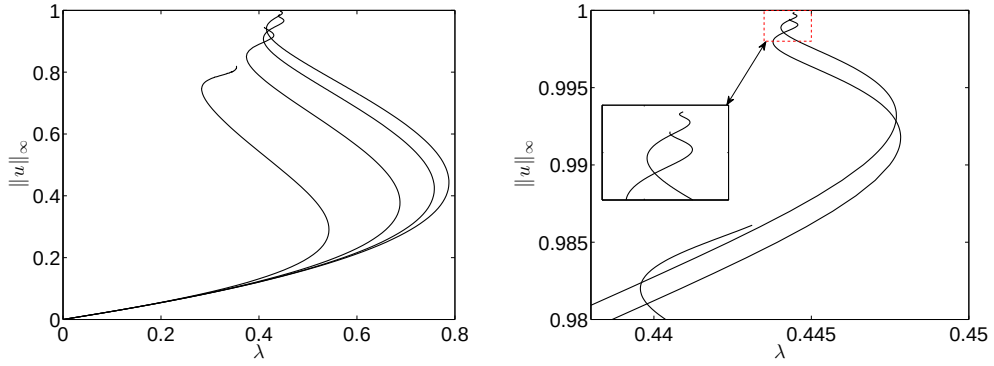

(a) (b) Zoomed

FIGURE 3. (a) Bifurcation curves of (1.1) in $B_1(0)$ computed via numerics for various ε. From right to left, the curves correspond to $\varepsilon = 0.05, 0.1, 0.5, 1, 2$. At this scale $\varepsilon = 0.05$ and $\varepsilon = 0.1$ appear equal. (b) A magnified portion of (a). Here, the curves for $\varepsilon = 0.05, 0.1, 0.5$ are seen.

(λ_*, α_*), the value of the derivative of the solution (in the radial direction) becomes unbounded at some internal point, thus characterizing this bifurcation point as a blow-up in the gradient. Additionally, it suggests that multivalued solutions may be continued beyond the dead-end point.

To investigate this latter observation, we assume that the dimensionless equilibrium deflection of the membrane is defined parametrically by $(x(a,b), y(a,b), z(a,b))$ for local coordinates (a,b), instead of the more restrictive non-parametric form $(x, y, u(x,y))$. In this way, the new problem for (1.1) becomes

$$2H/\varepsilon = \frac{\lambda}{(1+z)^2} \quad \text{on } \Sigma, \tag{1.4 a}$$

$$(x,y) = \partial\Omega \ \text{ on } \partial\Sigma, \qquad z = 0 \ \text{ on } \partial\Sigma, \tag{1.4 b}$$

where the surface Σ is defined the by the map $X(a,b;\varepsilon) = (x(a,b), y(a,b), \varepsilon z(a,b))$ and H

is its mean curvature. Consequently, this generalization removes the difficulties encountered at vertical tangents and allows for the bifurcation curve of (1.1) to be a continued beyond the dead-end point.

In the particular case of Ω equal to the unit ball $B_1(0)$ in $\mathbb{R}^2$, we show that by taking advantage of radially symmetry, problem (1.4) reduces to the coupled system of ODEs

$$\begin{aligned} &r'' = -\frac{\varepsilon^2\lambda z'}{(1+z)^2} + \frac{\varepsilon^2 (z')^2}{r}, \qquad z'' + \frac{r'z'}{r} = \frac{\lambda r'}{(1+z)^2}, \qquad 0 < s < \ell; \\ &r(0) = 0, \quad r'(0) = 1, \quad r(\ell) = 1, \quad z'(0) = 0, \quad z(\ell) = 0, \end{aligned} \tag{1.5}$$

where ℓ is the length of the curve $(r(s), \varepsilon z(s))$ and is to be determined. Then we perform a singular perturbation analysis of (1.5) in the limit as $z(0) \to -1^+$ to recover an infinite fold point structure that is similar to that of (1.3) in $B_1(0)$ (see Figures 4(a)–(b)). However, all of the additional solutions beyond (λ_*, α_*) cannot be put into nonparametric form, *i.e.*, they cannot be represented as the graph of a function $z = u(x, y)$ in $B_1(0)$ (cf. [1]). We call these solutions *strictly parametric*.

The disappearance of solutions behavior is not isolated to problem (1.1) and has arisen in other mean curvature equations [5, 8, 15, 16]. In addition, issues of existence, uniqueness and multiplicity of solutions to problems of general type

$$\operatorname{div} \frac{\nabla u}{\sqrt{1+|\nabla u|^2}} = \lambda f(x,u), \quad x \in \Omega; \qquad u = 0, \quad x \in \partial\Omega$$

have been a topic of recent consideration by several authors (see [3, 12, 17, 18, 19] and the references there-in). Our main results are now stated.

1.1 Statement of main results

First, in §2.1, we establish the following necessary condition for the existence of solutions of problem (1.1) in the unit ball.

Theorem 2.3 *Fix $\varepsilon > 0$ and let $u(\cdot\,;\lambda)$, with $\lambda > 0$, be a solution to problem (1.1) in the two-dimensional unit ball $B_1(0)$. Then $\|u\|_\infty \leqslant 1 - B(\varepsilon^2\lambda)$, where B is defined as*

$$B(\Lambda) := \begin{cases} \dfrac{\left(3-2\sqrt{2}\right)}{2}\Lambda, & \text{when} \quad 0 < \Lambda \leqslant 4 + 3\sqrt{2}, \\ \dfrac{3\Lambda + \sqrt{\Lambda(\Lambda-8)}}{4(1+\Lambda)}, & \text{when} \quad \Lambda > 4 + 3\sqrt{2}. \end{cases} \tag{2.6}$$

Consequently, for any $\lambda < \lambda^*$ and $\varepsilon > 0$, there exists an $\alpha_*(\varepsilon, \lambda) \in \mathbb{R}$ such that $\|u\|_\infty < \alpha_* < 1$.

This result is proved in the Lemmas and Theorems leading up to Corollary 2.4 and demonstrates that unlike problem (1.3), problem (1.1) in $B_1(0)$ has no solutions for $\|u\|_\infty$ arbitrarily close to 1. This loss of a classical solution is shown to be due to the formation of a singularity in the radial derivative at a point internal to the domain.

Next to complement the aforementioned qualitative result, we employ a novel formal asymptotic analysis to gain insight into the disappearance of solutions at the *dead-end*

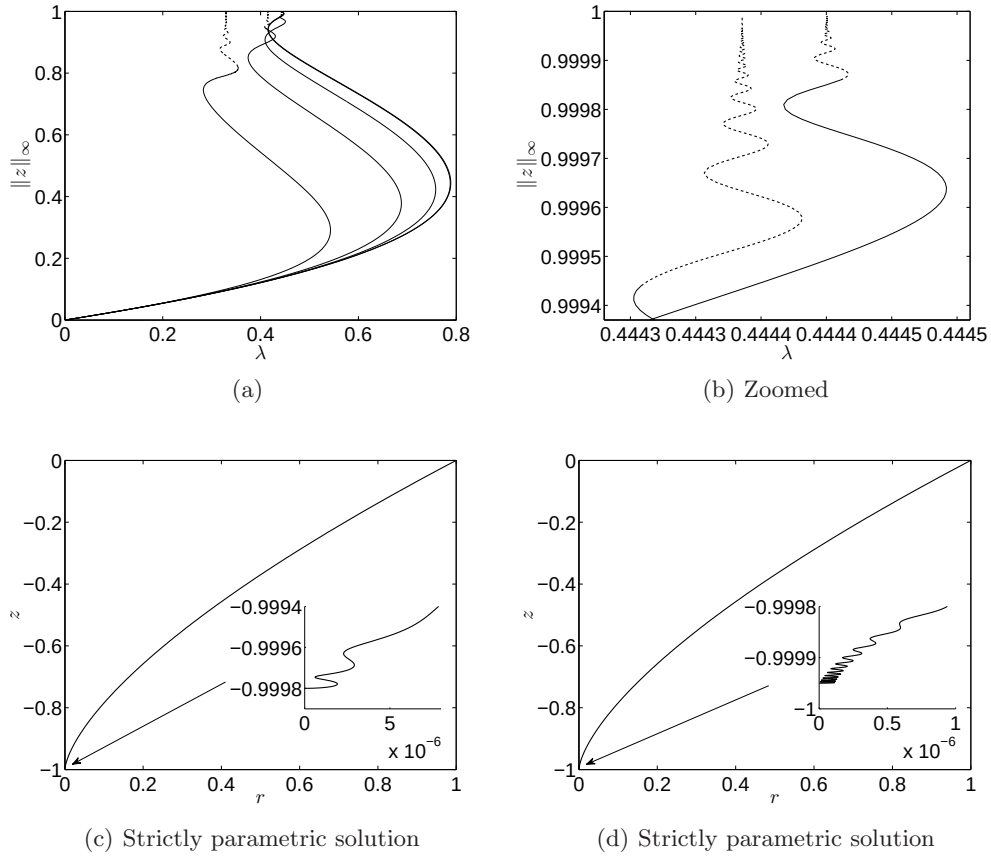

(a) (b) Zoomed

(c) Strictly parametric solution (d) Strictly parametric solution

FIGURE 4. (a) Bifurcation curves of (1.5) computed via numerics for various ε. The dashed line represents *strictly parametric solutions*, which naturally continue on from the final classical solutions of (1.1). From right to left, the curves correspond to $\varepsilon = 0.05, 0.1, 0.5, 1, 2$. (b) A magnified portion of panel (a), where $\varepsilon = 0.05, 0.1$, correspond to the right and left curves, respectively. In panels (c) and (d), the radially symmetric solutions from the strictly parametric branch are plotted for the case $\varepsilon = 0.1$ with $z(0) = -0.9998$ and $z(0) = -0.99995$, respectively. As indicated by the insets displaying a zoomed neighbourhood of the origin, the solution is multivalued and folds back upon itself multiple times. As the branch is traversed, solutions undergo additional folding.

point and establish a very accurate prediction of its location. Our analysis demonstrates that the disappearance of solutions is connected in an intricate way to small values of the parameters ε and $\delta := 1 - \|u\|_\infty$. Therefore, the perturbation analysis involves two small parameters and must be performed in the distinguished limit $\varepsilon^2/\delta = \delta_0$ for $\delta_0 = \mathcal{O}(1)$. This formal approach allows for an explicit characterization of the upper solution branch in terms of two functions. Formally, we obtain the following result.

Principal Result 2.1 *For solutions u of* (1.1) *in the two-dimensional unit ball $B_1(0)$, there is a regime where both $\varepsilon \ll 1$ and $\delta \ll 1$, with $\varepsilon^2/\delta = \mathcal{O}(1)$, such that the upper*

solution branch of the bifurcation curve has the asymptotic parameterization

$$\|u\|_\infty = 1-\delta, \qquad \lambda = \frac{4}{9} - \delta\frac{4}{3}\tilde{A}(\varepsilon^2/\delta)\sin\left[-\sqrt{2}\log\delta + \tilde{\phi}(\varepsilon^2/\delta)\right] + \mathcal{O}(\delta^2) \tag{1.6}$$

as $\delta \to 0^+$*, where* $\tilde{A}(\delta_0)$ *and* $\tilde{\phi}(\delta_0)$ *are functions determined by the initial value problem*

$$\frac{1}{\rho}\left(\frac{\rho {w_0}'}{\sqrt{1+\delta_0 {w_0}'^2}}\right)' = \frac{4}{9}{w_0}^{-2}, \quad 0<\rho<\infty; \qquad w_0(0)=1,\ {w_0}'(0)=0 \tag{1.7 a}$$

$$w_0 = \rho^{2/3} + \tilde{A}(\delta_0)\sin\left(\frac{2\sqrt{2}}{3}\log\rho + \tilde{\phi}(\delta_0)\right) + o(1) \qquad \rho\to\infty. \tag{1.7 b}$$

A casual inspection of expansion (1.6) may suggest that the result is uniformly valid as $\delta \to 0^+$, contradicting the results of Theorem 2.3. However, in Theorem 2.7 we prove that there exists a δ_0^* such that initial value problem (1.7) has no global solutions when $\delta_0 \geqslant \delta_0^*$. This implies that (1.6) is only valid for $\varepsilon^2/\delta < \delta_0^*$, and the value of δ_0^* can then be used to accurately predict the dead-end point for problem (1.1) (see Principal Result 2.1).

Then in §2.3, nonparametric problem (1.4) with $\partial\Omega = B_1(0)$ is studied and found to be amenable to the aforementioned asymptotic analysis. In particular, an accurate representation of the solution branch in the limit $\delta := 1 + z(0) \to 0^+$ is obtained. Specifically, we have the formal result, which is uniformly valid as $\delta \to 0^+$.

Principal Result 2.3 *For solutions of problem* (1.4) *with* $\partial\Omega = B_1(0)$*, there is a regime where both* $\varepsilon \ll 1$ *and* $\delta \ll 1$*, with* $\varepsilon^2/\delta = \mathcal{O}(1)$*, such that the upper solution branch of the bifurcation curve has the asymptotic parameterization*

$$|z(0)| = 1-\delta, \qquad \lambda = \lambda_0 - \delta\,\frac{4}{3}\,\tilde{A}_1(\varepsilon^2/\delta)\sin\left[-\sqrt{2}\log\delta + \tilde{\phi}_1(\varepsilon^2/\delta)\right] + \mathcal{O}(\delta^2). \tag{1.8}$$

Moreover, $\lambda_0 = 4/9$*, and the functions* $\tilde{A}_1(\delta_0)$ *and* $\tilde{\phi}_1(\delta_0)$ *are determined by the far field behavior of* Z_0*,*

$$Z_0(\rho) = \rho^{2/3} - \frac{4\delta_0}{9} + \tilde{A}_1(\delta_0)\sin\left(\frac{2\sqrt{2}}{3}\log\rho + \tilde{\phi}_1(\delta_0)\right) + o(1) \quad \text{as } \rho\to\infty, \tag{1.9 a}$$

of the initial value problem

$$\begin{aligned} &{R_0}'' = -\frac{4\delta_0}{9}\frac{{Z_0}'}{{Z_0}^2} + \delta_0\frac{({Z_0}')^2}{R_0}, \qquad {Z_0}'' + \frac{{R_0}'{Z_0}'}{R_0} = \frac{4}{9}\frac{{R_0}'}{{Z_0}^2}, \qquad 0<\rho<\infty; \\ &R_0(0)=0, \quad {R_0}'(0)=1, \quad Z_0(0)=1, \quad {Z_0}'(0)=0, \end{aligned} \tag{1.9 b}$$

where

$$R_0(\rho) = \rho - \frac{2\delta_0}{3}\rho^{1/3} + o(1) \quad \text{as } \rho\to\infty. \tag{1.9 c}$$

This result shows that nonparametric problem (1.4) provides a natural continuation to solutions of problem (1.1) beyond the dead-end point. These additional solutions are found to be strictly parametric, as seen in Figure 4(c) and Figure 4(d).

Last, in §3, a few open problems are discussed.

2 Two-dimensional analysis

2.1 A necessary condition for existence of solutions

In this section, we investigate the disappearance of classical solutions u of problem (1.1) in $B_1(0)$ using techniques similar to ones introduced in [4, 8] to study the behavior of pendent liquid drops. To do so we first note that since the right-hand side of equation (1.1 *a*) is positive, the solutions to problem (1.1) must be negative (see, e.g., [9, 21]). From this fact we can apply a Gidas-Ni-Nirenberg type result to infer that u is necessarily radially symmetric [22, Thm. 8.2.1]. That is, $u(x, y) = u(r)$, where $r = \sqrt{x^2 + y^2}$, and problem (1.1) in the unit ball $B_1(0)$ reduces to

$$\frac{1}{r}\left(\frac{ru'}{\sqrt{1+\varepsilon^2 u'^2}}\right)' = \frac{\lambda}{(1+u)^2}, \quad 0 < r < 1; \quad u'(0) = u(1) = 0, \tag{2.1}$$

where $u(r) \in (-1, 0]$ for $0 < r < 1$. For convenience, we introduce the change of variable $u(r) \mapsto u(\rho = r/\varepsilon)$, which from problem yields

$$\frac{1}{\rho}\left(\frac{\rho u'}{\sqrt{1+u'^2}}\right)' = \frac{\Lambda}{(1+u)^2}, \quad 0 < \rho < \varepsilon^{-1}; \qquad u'(0) = 0,\ u(\varepsilon^{-1}) = 0. \tag{2.2}$$

Here, $'$ now represents differentiation with respect to ρ, and $\Lambda := \varepsilon^2\lambda$. In this form, the ordinary differential equation in (2.2) admits the very advantageous geometrical interpretation:

$$(\rho \sin\psi)' = \frac{\Lambda\rho}{(1+u)^2},$$

where ψ is the angle of inclination of the solution curve (ρ, u), measured counterclockwise from the positive ρ-axis to its tangent. It is important to note that these differential equations are equivalent on any interval in which $|u'(\rho)| < \infty$.

Now to study the non-existence of solutions of (2.2), we look at the corresponding initial value problem

$$(\rho \sin\psi)' = \frac{\Lambda\rho}{(1+u)^2}, \quad \rho > 0; \qquad u'(0) = 0,\ u(0) = \alpha \in (-1, 0), \tag{2.3}$$

whose *maximal interval of existence* is $[0, \rho_1)$. Note that $\rho_1 \in (0, +\infty]$; however, in what follows, we will show that for a certain range of α sufficiently close to -1 the value of ρ_1 is finite, leading to the nonexistence of solutions of problem (2.2). To show this, we begin by proving the following lemma about solutions of initial value problem (2.3).

Lemma 2.1 *If u is a solution of initial value problem* (2.3) *in* $[0, \rho_1)$*, then* $\sin\psi > 0$ *in* $(0, \rho_1)$*, which implies that u is increasing on that interval. Furthermore, we have the following bound for ρ in* $(0, \rho_1)$*:*

$$\frac{\Lambda}{2(1+u(\rho))^2} < \frac{\sin\psi}{\rho} < \frac{\Lambda}{2(1+\alpha)^2}. \tag{2.4}$$

Proof An integration of the differential equation in problem (2.3) yields

$$\sin\psi = \frac{\Lambda}{\rho}\int_0^\rho \frac{\xi}{(1+u(\xi))^2}\,\mathrm{d}\xi > 0, \quad \rho \in (0, \rho_1). \tag{2.5}$$

Now since u is increasing on $(0,\rho_1)$, we have $\alpha < u(\rho) < u(\rho_1)$ for $\rho \in (0,\rho_1)$, and the equality in (2.5) gives inequality (2.4). □

Next we prove a crucial lemma about the solutions of initial value problem (2.3).

Lemma 2.2 *Let $\Lambda > 0$ and assume that $u(\rho;\Lambda)$ is a solution to problem (2.3), whose maximal interval of existence is $[0,\rho_1)$. If $\alpha < -1 + B(\Lambda)$, where*

$$B(\Lambda) := \begin{cases} \dfrac{\left(3-2\sqrt{2}\right)}{2}\Lambda, & \text{when} \quad 0 < \Lambda \leqslant 4+3\sqrt{2}, \\ \dfrac{3\Lambda + \sqrt{\Lambda(\Lambda-8)}}{4(1+\Lambda)}, & \text{when} \quad \Lambda > 4+3\sqrt{2}, \end{cases} \tag{2.6}$$

then ρ_1 is finite. In particular,

$$\frac{2(1+\alpha)^2}{\Lambda} < \rho_1 \leqslant \frac{2\,(1+M)^2}{\Lambda}. \tag{2.7 a}$$

Moreover, at the end point (ρ_1, u_1), where $u_1 := \lim_{\rho\to\rho_1^-} u(\rho)$, we have the bound

$$\alpha + \frac{2(1+\alpha)^2}{\Lambda} < u_1 < M < 0. \tag{2.7 b}$$

and $u' \to +\infty$ as $\rho \to \rho_1^-$, i.e., the slope of u becomes vertical at $\rho = \rho_1$. Here, M is specifically defined as

$$M := \frac{\Lambda(1+3\alpha) - 2(1+\alpha)^2 - (1+\alpha)\sqrt{\Lambda^2 - 12\Lambda(1+\alpha) + 4(1+\alpha)^2}}{2\Lambda}, \tag{2.8}$$

Proof Assume, for contradiction, that there exists a value ρ in $(0,\rho_1)$ such that $u(\rho) = M$, where M is defined in (2.8). Note that since $\alpha < -1 + B(\Lambda)$, the value $M \in (-\alpha, 0)$. First, we have that because u is a solution of problem (2.3),

$$\frac{\sin\psi}{\rho} + (\sin\psi)' = \frac{\Lambda}{(1+u)^2}, \quad \rho \in (0,\rho_1). \tag{2.9}$$

Moreover, by Lemma 2.1, the solution u is increasing on this interval and we may use it as independent variable; thus using

$$\frac{\mathrm{d}}{\mathrm{d}\rho}(\sin\psi) = -\frac{\mathrm{d}}{\mathrm{d}u}(\cos\psi), \tag{2.10}$$

in equation (2.9) and then integrating the result with respect to u, we obtain

$$\frac{\Lambda}{2(1+\alpha)^2}(u-\alpha) + (1-\cos\psi(u)) > \Lambda\left[\frac{1}{1+\alpha} - \frac{1}{1+u}\right],$$

where we have used inequality (2.4); or, equivalently

$$1 - \cos\psi(u) > \frac{\Lambda(u-\alpha)}{(1+\alpha)(1+u)} - \frac{\Lambda(u-\alpha)}{2(1+\alpha)^2}. \tag{2.11}$$

Then from this inequality and a comparison principle, we have our desired result (cf. [4, §2] or [8, §4.6]). □

Therefore, we have that if $u(\cdot\,;\alpha)$ is a solution to (2.3), with $\alpha < -1 + B(\Lambda)$, then its derivative blows-up in finite time. Furthermore, from the definition of B in (2.6), the blow-up point (ρ_1, u_1) must happen for $u_1 < 0$. In using this crucial fact, we can establish the following theorem, which rigorously proves, for all $\varepsilon > 0$, the disappearing solution behavior of problem (1.1) in $B_1(0)$ observed in [1].

Theorem 2.3 *Fix $\varepsilon > 0$ and let $u(\cdot\,;\lambda)$, with $\lambda > 0$, be a solution to problem* (1.1) *in the two-dimensional unit ball $B_1(0)$. Then $\|u\|_\infty \leqslant 1 - B(\varepsilon^2\lambda)$, where B is defined in* (2.6).

Proof Because u is a solution of problem (1.1) in $B_1(0)$, we have that it is radially symmetric and increasing with respect to r (see Lemma 2.1), implying $u(0) = -\|u\|_\infty$. Furthermore, $u(r/\varepsilon)$ is a solution of problem (2.2), which in turn is a solution of problem (2.3) on $(0, \rho_1)$, with $\rho_1 \geqslant 1/\varepsilon$. Assuming $\|u\|_\infty > 1 - B(\varepsilon^2\lambda)$, i.e., $u(0) < -1 + B(\varepsilon^2\lambda)$, we obtain that $u|_{\partial B_1(0)} \leqslant u(\rho_1) < 0$, which is a contradiction. Therefore, this assumption must be wrong, which implies that $\|u\|_\infty \leqslant 1 - B(\varepsilon^2\lambda)$. □

An immediate corollary to this theorem is the following.

Corollary 2.4 *Let $\varepsilon > 0$ be fixed and $\lambda > 0$. Then there exists an $\alpha_*(\varepsilon, \lambda) < 1$ such that if $u(\cdot\,;\lambda)$ is a solution of problem* (1.1) *in $B_1(0)$, then $\|u\|_\infty < \alpha_*$.*

An illustration of Theorem 2.3 is shown in Figure 5.

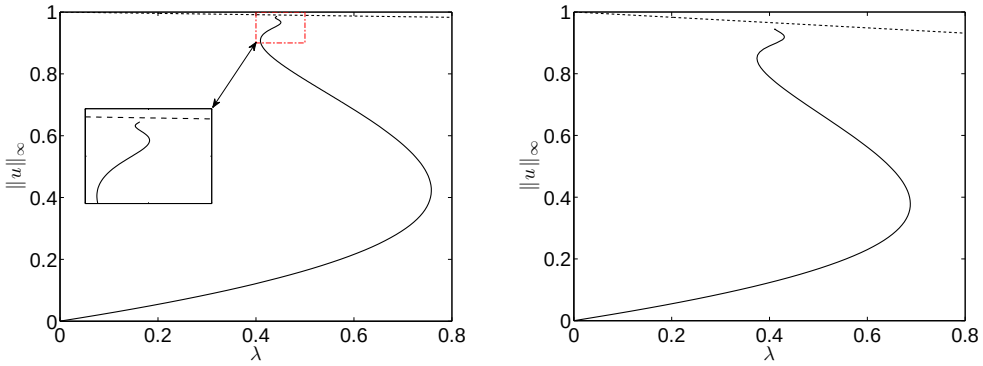

(a) $\varepsilon = 0.5$ (b) $\varepsilon = 1$

FIGURE 5. An illustration of Theorem 2.3. On or below the dashed line is the region where $\|u\|_\infty$ must be, if u is a solution of problem (1.1) in $B_1(0)$. As seen, this region keeps the bifurcation diagram bound away from $\|u\|_\infty = 1$. (a) For $\varepsilon = 0.5$; (b) For $\varepsilon = 1$.

2.2 Asymptotic analysis

In this section, we develop a novel singular perturbation technique to analyze the upper solution branch of problem (1.1) in the two-dimensional unit ball for $\varepsilon \ll 1$. To this end,

we consider the equation

$$\frac{1}{r}\left(\frac{ru'}{\sqrt{1+\varepsilon^2 u'^2}}\right)' = \frac{\lambda}{(1+u)^2}, \quad 0<r<1; \qquad u'(0)=u(1)=0, \tag{2.1}$$

in the limits $\varepsilon \to 0^+$ and $\delta \to 0^+$, where $\delta := 1 - \|u\|_\infty = 1 + u(0)$. The analysis will reveal that these two small parameters must be related together in order to facilitate the matching. In these limits, (2.1) is a singular perturbation problem with an inner layer at $r = 0$. Therefore, in the outer region away from $r = 0$, we expand u and λ as

$$u = u_0 + \varepsilon^2 u_1 + \mathcal{O}(\varepsilon^4), \qquad \lambda = \lambda_0 + \varepsilon^2 \lambda_1 + \mathcal{O}(\varepsilon^4), \tag{2.12}$$

and gather terms of similar order to find

$$\Delta u_0 = \frac{\lambda_0}{(1+u_0)^2}, \qquad u_0(0) = -1, \quad u_0(1) = 0, \tag{2.13 a}$$

$$\Delta u_1 + \frac{2\lambda_0}{(1+u_0)^3}u_1 = \frac{\lambda_1}{(1+u_0)^2} + \frac{3\lambda_0 (u_0{}')^2}{2(1+u_0)^2} - \frac{(u_0{}')^3}{r}, \qquad u_1(1) = 0. \tag{2.13 b}$$

Here, $\Delta := \partial_{rr} + r^{-1}\partial_r$ denotes the two-dimensional radial Laplacian. The general solution of problem (2.13) is

$$u_0 = -1 + r^{2/3}, \quad \lambda_0 = \frac{4}{9}; \qquad u_1 = \frac{\lambda_1}{3\lambda_0} r^{2/3} + A\sin(\omega \log r + \phi) \tag{2.14}$$

for constants A, ϕ—which will be determined by matching—and $\omega := (2\sqrt{2})/3$. Note that $u_0{}'$ is not finite at $r = 0$, so the condition $u'(0) = 0$ will need to be enforced in a boundary layer centered around $r = 0$. The value of λ_1 will eventually be fixed by the boundary condition $u_1(1) = 0$.

Next we analyze the boundary layer near $r = 0$ by introducing the inner variables

$$\rho = r/\gamma, \qquad u = -1 + \delta w(\rho),$$

where $\gamma \ll 1$ is the scale of the boundary layer. Substituting these change of variables into problem (2.1) gives the following equation for $w(\rho)$:

$$\frac{1}{\rho}\left(\frac{\rho w'}{\sqrt{1+\varepsilon^2\delta^2\gamma^{-2}w'^2}}\right)' = \frac{\gamma^2}{\delta^3}\frac{\lambda}{w^2}, \quad 0<\rho<\infty; \qquad w(0)=1,\ w'(0)=0.$$

A dominant balance requires that $\gamma = \delta^{3/2}$ and $\varepsilon^2/\delta = \delta_0$, where δ_0 is an $\mathcal{O}(1)$ constant. Then we expand w as $w = w_0 + o(1)$, for $\delta \to 0^+$, and find that the problem for $w_0(\rho)$ is

$$\frac{1}{\rho}\left(\frac{\rho w_0{}'}{\sqrt{1+\delta_0 w_0{}'^2}}\right)' = \frac{\lambda_0}{{w_0}^2}, \quad 0<\rho<\infty; \qquad w_0(0)=1,\ w_0{}'(0)=0. \tag{2.15}$$

The matching condition, from (2.14), provides the leading order far field behavior $w_0 \sim \rho^{2/3}$ as $\rho \to \infty$. To find the next order correction, we look for perturbations about this leading order form. Specifically, we let $w_0 = \rho^{2/3} + v(\rho) + \cdots$ as $\rho \to \infty$, where $v \ll \rho^{2/3}$, and retain all the linear terms to obtain

$$\Delta v + \frac{2\lambda_0}{\rho^2}v + \frac{2\delta_0}{\rho^{4/3}}v' = 0,$$

which via WKB analysis has the far field behavior

$$v \sim \tilde{A}(\delta_0)\sin(\omega\log\rho + \tilde{\phi}(\delta_0)), \qquad \text{as } \rho \to \infty.$$

Therefore, the function $w_0 \sim \rho^{2/3} + v + \cdots$ as $\rho \to \infty$, which augments problem (2.15) to give the full specification of w_0:

$$\frac{1}{\rho}\left(\frac{\rho {w_0}'}{\sqrt{1+\delta_0 {w_0}'^2}}\right)' = \frac{\lambda_0}{{w_0}^2}, \quad 0<\rho<\infty; \qquad w_0(0)=1,\ {w_0}'(0)=0, \tag{2.16 a}$$

$$w_0 \sim \rho^{2/3} + \tilde{A}(\delta_0)\sin(\omega\log\rho + \tilde{\phi}(\delta_0)), \qquad \text{as} \qquad \rho\to\infty. \tag{2.16 b}$$

To carry out matching, we introduce the intermediate variable $r_\eta = r/\eta(\varepsilon)$, where $\varepsilon^3 \ll \eta \ll 1$ as $\varepsilon \to 0^+$, and the corresponding order $\mathcal{O}(\varepsilon^2)$ condition

$$\lim_{\substack{\varepsilon\to 0^+ \\ r_\eta \text{ fixed}}} \frac{1}{\varepsilon^2}\left(u_0(\eta r_\eta) + \varepsilon^2 u_1(\eta r_\eta) + 1 - \frac{\varepsilon^2}{\delta_0} w_0({\delta_0}^{3/2}\eta r_\eta/\varepsilon^3)\right) = 0. \tag{2.17}$$

From solution (2.14) and problem (2.16) we have

$$\begin{aligned}
\frac{1}{\varepsilon^2}u_0(\eta r_\eta) &= -\frac{1}{\varepsilon^2} + \frac{\eta}{\varepsilon^2}{r_\eta}^{2/3} \\
u_1(\eta r_\eta) &= \frac{\lambda_1}{3\lambda_0}\eta^{2/3}{r_\eta}^{2/3} + A\sin(\omega\log\eta r_\eta + \phi) \\
\frac{1}{\delta_0}w_0\left(\frac{{\delta_0}^{3/2}\eta r_\eta}{\varepsilon^3}\right) &= \frac{\eta^{2/3}}{\varepsilon^2}{r_\eta}^{2/3} + \frac{\tilde{A}(\delta_0)}{\delta_0}\sin(\omega\log(\eta r_\eta) + \omega\log\frac{{\delta_0}^{3/2}}{\varepsilon^3} + \tilde{\phi}(\delta_0)) + o(1)
\end{aligned}$$

as $\varepsilon \to 0^+$, where r_η is fixed, so that equation (2.17) yields

$$A = \frac{\tilde{A}(\delta_0)}{\delta_0}, \qquad \phi = \omega\log({\delta_0}^{3/2}/\varepsilon^3) + \tilde{\phi}(\delta_0).$$

Finally applying the boundary condition $u_1(1) = 0$ in (2.14) gives

$$\lambda_1 = -3\lambda_0\frac{\tilde{A}(\delta_0)}{\delta_0}\sin(\omega\log({\delta_0}^{3/2}/\varepsilon^3) + \tilde{\phi}(\delta_0))$$

and hence,

$$\lambda = \lambda_0 + \varepsilon^2\lambda_1 + \mathcal{O}(\varepsilon^4) = \lambda_0 - \delta 3\lambda_0\tilde{A}(\delta_0)\sin(-\sqrt{2}\log\delta + \tilde{\phi}(\delta_0)).$$

At this stage, we fix the value of ε in the main problem (2.1) and write $\delta_0 = \varepsilon^2/\delta$ with ε^2 fixed but still $\mathcal{O}(\delta)$. This leads to the following asymptotic result regarding the upper solution branch of the bifurcation curve for problem (1.1) in $B_1(0)$.

Principal Result 2.1 *For solutions u of problem* (1.1) *in the two-dimensional unit ball $B_1(0)$, there is a regime where both $\varepsilon \ll 1$ and $\delta \ll 1$, with $\varepsilon^2/\delta = \mathcal{O}(1)$, such that the upper solution branch of the bifurcation curve has the asymptotic parameterization*

$$\|u\|_\infty = 1-\delta, \qquad \lambda = \frac{4}{9} - \delta\frac{4}{3}\tilde{A}(\varepsilon^2/\delta)\sin\left[-\sqrt{2}\log\delta + \tilde{\phi}(\varepsilon^2/\delta)\right] + \mathcal{O}(\delta^2). \tag{2.18}$$

where $\tilde{A}(\delta_0)$ and $\tilde{\phi}(\delta_0)$ are functions determined by the initial value problem

$$\frac{1}{\rho}\left(\frac{\rho {w_0}'}{\sqrt{1+\delta_0({w_0}')^2}}\right)' = \frac{4}{9}\frac{1}{w_0^2}, \quad 0<\rho<\infty; \qquad w_0(0)=1,\ {w_0}'(0)=0 \tag{2.19 a}$$

$$w_0 = \rho^{2/3} + \tilde{A}(\delta_0)\sin\left(\frac{2\sqrt{2}}{3}\log\rho + \tilde{\phi}(\delta_0)\right) + \mathcal{O}(1) \qquad \rho\to\infty. \tag{2.19 b}$$

The asymptotic parameterization (2.18) of the upper solution branch of (2.1) appears outwardly to be defined for $\|u\|_\infty$ arbitrarily close to 1, potentially contradicting Corollary 2.4. However, the parameterization assumes that the quantities $\tilde{A}(\varepsilon^2/\delta)$ and $\tilde{\phi}(\varepsilon^2/\delta)$ are well defined as $\delta\to 0^+$. So one can expect that $\tilde{A}(\delta_0)$ and $\tilde{\phi}(\delta_0)$ will not be defined for δ_0 sufficiently large. Therefore before observing the predictive accuracy of (2.18), let us first consider the existence of solutions to (2.19 *a*) for δ_0 sufficiently large.

To do so, we follow a similar procedure to the one outlined in the previous section and introduce a change of variables—specifically, $\xi = \rho/\sqrt{\delta_0}$, with $w_0(\rho) = v(\xi)$—so that problem (2.19 *a*) becomes

$$\frac{1}{\xi}\left(\frac{\xi v'}{\sqrt{1+(v')^2}}\right)' = \frac{4\delta_0}{9}\frac{1}{v^2}, \quad 0<\xi<\infty; \qquad v(0)=1,\ v'(0)=0. \tag{2.20}$$

Hence, the mean curvature operator is isolated on the left-hand side, and the differential equation in problem (2.20) yields the geometric representation

$$\frac{(\xi\sin\psi)'}{\xi} = \frac{4\delta_0}{9}\frac{1}{v^2}, \tag{2.21 a}$$

where ψ is the angle of inclination of the solution curve. In noting that the differential equation in problem (2.20) and differential equation (2.21 *a*) are equivalent on any interval in which $v'(\xi)$ is bounded, we look at (2.21 *a*), coupled with the initial condition

$$v(0) = 1, \tag{2.21 b}$$

to study the nonexistence of solutions of problem (2.20). Also note that if v satisfies problem (2.21), then the condition $v'(0)=0$ is redundant, which can be seen by integrating differential equation (2.21 *a*) and then taking $\xi\to 0^+$. Futhermore, we set $[0,\Xi)$ to be the *maximal interval of existence* of initial value problem (2.21) and like in §2.1, show that Ξ must be finite when δ_0 is sufficiently large.

Lemma 2.5 *If v satisfies initial value problem* (2.21) *on $[0,\Xi)$, then $\sin\psi > 0$ for $\xi\in(0,\Xi)$, which implies that v is increasing on that interval. Furthermore, we have the following bound for ξ in $(0,\Xi)$:*

$$\frac{2\delta_0}{9v(\xi)^2} < \frac{\sin\psi(\xi)}{\xi} < \frac{2\delta_0}{9}. \tag{2.22}$$

Proof Integrating differential equation (2.21 *a*) yields

$$\sin\psi(\xi) = \frac{4\delta_0}{9}\frac{1}{\xi}\int_0^\xi \eta\ v(\eta)^{-2}\,\mathrm{d}\eta > 0.$$

for all ξ in $(0,\Xi)$, and the results follow as in Lemma 2.1. □

Now, we can prove the main lemma which leads to our desired main result for the nonexistence of solutions of problem (2.19 *a*).

Lemma 2.6 *Assume that v is a solution of initial value problem (2.21 a) with $v(0) = 1$, whose maximal interval of existence is $[0,\Xi)$. If*

$$\delta_0 \geqslant \bar{\delta}_0 := \frac{9(2\sqrt{2}+3)}{2}, \tag{2.23}$$

then Ξ and $V := \lim_{\xi\to\Xi^-} v(\xi)$ must satisfy

$$\frac{9}{2\delta_0} < \xi_1 \leqslant \frac{9}{2\delta_0}\bar{M}^2 \quad \textit{and} \quad 1 + \frac{9}{2\delta_0} < V < \bar{M}, \tag{2.24}$$

respectively, where

$$\bar{M} := \frac{3(2\delta_0 - 3) - \sqrt{4\delta_0(\delta_0 - 27) + 81}}{4\delta_0} > 1. \tag{2.25}$$

Moreover, $v' \to +\infty$ as $\xi \to \Xi^-$, i.e., v' blows-up in finite time.

Proof Assume for contradiction that there exist a value ξ in $(0,\Xi)$ such that $v(\xi) = \bar{M}$. First by Lemma 2.5, we know that on $(0,\Xi)$ the solution v is increasing and consequently, may use it as the independent variable; thus equation (2.21 *a*) gives

$$\frac{\sin\psi}{\xi} - (\cos\psi)_v = \frac{4\delta_0}{9}\frac{1}{v^2}, \tag{2.26}$$

Then integrating with respect to v and using inequality (2.22) yields

$$1 - \cos\psi(v) > \frac{4\delta_0}{9}\left(1 - \frac{1}{v}\right) - \frac{2\delta_0}{9}(v-1),$$

or

$$\frac{2\delta_0}{9}\left(v + \left[\frac{9}{2\delta_0} - 3\right] + \frac{2}{v}\right) > \cos\psi(v);$$

Then, as in proof of Lemma 2.2, the final results follow from this inequality and a comparison theorem (see again [4, §2] or [8, §4.6]). □

Therefore, since problem (2.21) and problem (2.20) are equivalent on $(0,\xi_1)$, then the derivative of problem (2.20) also blows-up in finite time, which after changing variables back to ρ yields the following result concerning initial value problem (2.19 *a*).

Theorem 2.7 *There exists a value δ_0^* such that for $\delta_0 \geqslant \delta_0^*$ no global solutions of initial*

value problem (2.19 *a*) *exist. Furthermore,*

$$\delta_0^* \leqslant \bar{\delta}_0 := \frac{9(2\sqrt{2}+3)}{2} \approx 26.2279.$$

Remark A numerical integration of the initial value problem (2.19 *a*) gives $\delta_0^* \approx 18.142468$, indicating that $\bar{\delta}_0$ is not a particularly tight upper bound on δ_0^*.

As a result of this theorem, an expansion for the dead-end point $(\lambda_*(\varepsilon), \alpha_*(\varepsilon))$ can now be extracted from (2.18); specifically, since problem (2.19 *a*) has no solutions for $\delta_0 \geqslant \delta_0^*$, the asymptotic approximation (2.18) fails at $\varepsilon^2/\delta = \delta_0^*$, or $\delta = \varepsilon^2/\delta_0^*$. Therefore using these values in (2.18), the following asymptotic result for the dead-point of problem (1.1) is established.

Principal Result 2.2 *For $\varepsilon \ll 1$, the dead-end point $(\lambda_*(\varepsilon), \alpha_*(\varepsilon))$ of the upper solution branch of the bifurcation curve of problem* (1.1) *in the two-dimensional unit ball $B_1(0)$ has the asymptotic expansion*

$$\begin{aligned} \alpha_*(\varepsilon) &= 1 - \varepsilon^2/\delta_0^* + \mathcal{O}(\varepsilon^4), \\ \lambda_*(\varepsilon) &= \frac{4}{9} - \varepsilon^2 \frac{4}{3} \frac{\tilde{A}(\delta_0^*)}{\delta_0^*} \sin\left[-\sqrt{2}\log(\varepsilon^2/\delta_0^*) + \tilde{\phi}\,(\delta_0^*)\right] + \mathcal{O}(\varepsilon^4). \end{aligned} \tag{2.27}$$

In order to study the quantitative accuracy of Principal Results 2.1 and 2.2, it is necessary to obtain the functions $\tilde{A}(\delta_0)$ and $\tilde{\phi}(\delta_0)$, which are readily acquired by solving problem (2.19 *a*) numerically, then subtracting off the growth term $\rho^{2/3}$ and applying a least squares fit to the remainder (see Figure 6). In Figure 7, comparisons of the full numerical solution of the upper branch of the bifurcation curve and asymptotic prediction of (2.18) are displayed; furthermore, the agreement is observed to be very good.

In Figure 8, a comparison of the numerical and asymptotic values for the location of the dead-end point is shown; note that agreement is very good, as in each case the asymptotic error is $\mathcal{O}(\varepsilon^4)$.

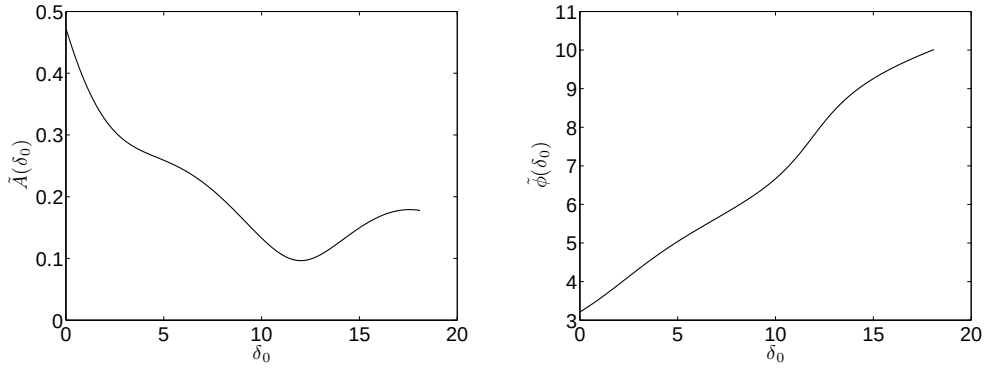

FIGURE 6. Graphs of $\tilde{A}(\delta_0)$ and $\tilde{\phi}(\delta_0)$ against δ_0. The numerical integration fails abruptly at roughly $\delta_0 = \delta_0^* \approx 18.142468$.

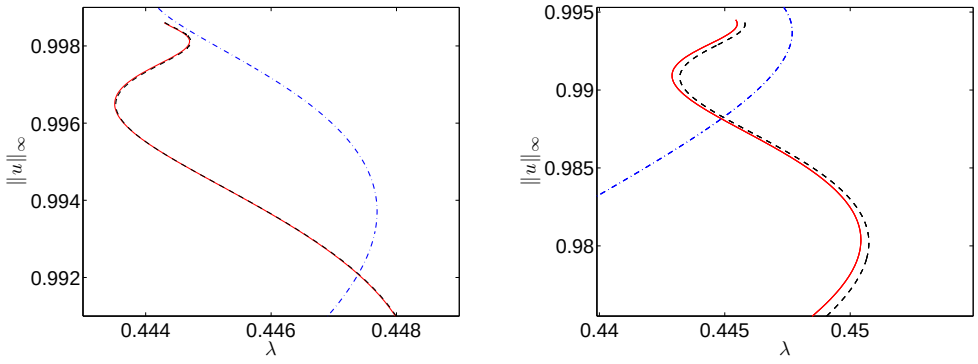

(a) $\varepsilon^2 = 0.025$ (b) $\varepsilon^2 = 0.1$

FIGURE 7. Comparison of the full numerical solution of the bifurcation curve for problem (1.1) in $B_1(0)$ (solid) with asymptotic formula (2.18) (dashed) and the solution curve of (1.1) in $B_1(0)$ for $\delta = 0$ (dash dot).

In Figure 9(a), the numerical (solid) and global asymptotic (dashed) solutions of problem (1.1) in $B_1(0)$ at the dead-end point (λ_*, α_*) for $\varepsilon^2 = 0.2$ are displayed. As expected (see §2.1), the tangent of the solution curve is almost vertitcal, indicating that the derivative of the solution is becoming unbounded. Indeed, when solutions $w_0{}'(\rho; \delta_0)$ of problem (2.19 *a*) are plotted for several δ_0 a blow-up in $w_0{}'(\rho; \delta_0)$, as $\delta_0 \to \delta_0^*$, is observed (see Figure 9(b)). This suggests that beyond the dead-end point solutions of (1.1) in $B_1(0)$ cannot be represented by a nonparametric function. Therefore, in the next section, problem (1.1) in $B_1(0)$ is put into parametric form, and consequently becomes a system of coupled ordinary differential equations. An asymptotic study of this coupled system reveals that strictly parametric solutions of problem (1.1) are present beyond the dead-end point of the bifurcation diagram.

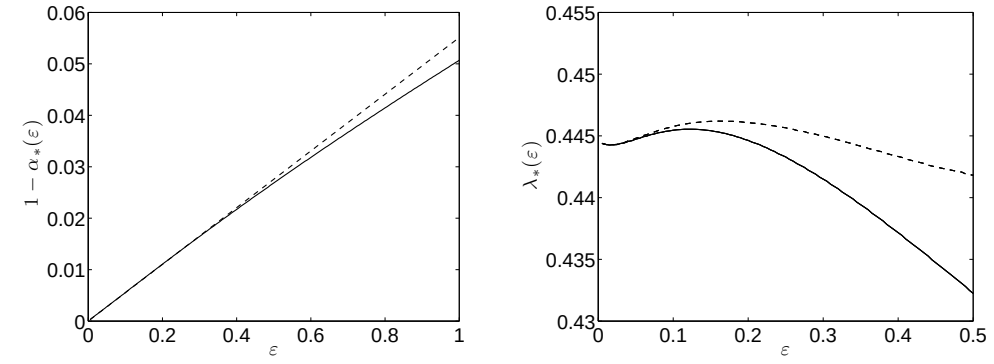

(a) $\varepsilon^2/\delta_0^* = 1 - \alpha_*(\varepsilon)$ (b) $\lambda_*(\varepsilon)$

FIGURE 8. Comparison of the asymptotic prediction, (2.27), (dashed line) of the dead end point $(\lambda_*(\varepsilon), \alpha_*(\varepsilon))$ with full numeric computations (solid) for: (a) the $\mathcal{O}(\varepsilon^2)$ correction of $\alpha_*(\varepsilon)$; (b) $\lambda_*(\varepsilon)$. Notice that the scale on the y-axis of the right figure is quite fine and so the agreement for $\lambda_*(\varepsilon)$ is in fact better than the figures makes it appear.

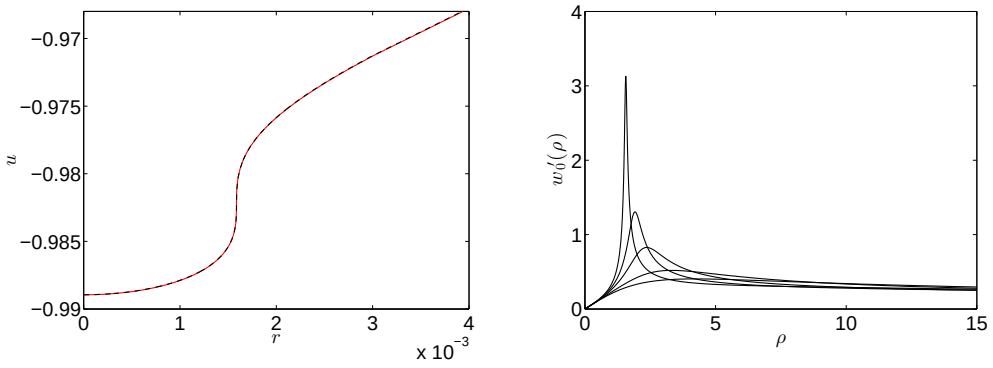

(a) Global Approximation for $\varepsilon^2 = 0.2$. (b) Blow up of $w_0'(\rho;\delta_0)$ as $\delta_0 \to \delta_0^*$.

FIGURE 9. (a) The numerical (solid) and global asymptotic (dashed) profile in the boundary layer. The curve is almost vertical indicating that the derivative is becoming infinite. (b) The derivative function $w_0'(\rho;\delta_0)$ plotted for several δ_0. As $\delta_0 \to \delta_0^*$, it observed that $w_0'(\rho;\delta_0)$ appears to develop a singularity at a finite ρ^*.

2.3 Arc length asymptotic analysis

In this section, we analyze the parametric problem, (1.4), for $\partial\Omega = \partial B_1(0)$, i.e.,

$$2H/\varepsilon = \frac{\lambda}{(1+z)^2} \quad \text{on } \Sigma, \tag{2.28 a}$$

$$(x,y) = \partial B_1(0) \ \text{ on } \partial\Sigma, \qquad z = 0 \ \text{ on } \partial\Sigma, \tag{2.28 b}$$

where the surface Σ is defined the by the map $X(a,b;\varepsilon) = (x(a,b), y(a,b), \varepsilon z(a,b))$ and H is its mean curvature. To simplify the situation, we first note that due to a result of Wente [23], the surface X must be rotationally symmetric about its vertical axis. Thus, X can be written as $X(s,\theta;\varepsilon) = (r(s)\cos\theta, r(s)\sin\theta, \varepsilon z(s))$, where $\theta \in [0, 2\pi)$ and s is the arc-length parameter of the curve $(r(s), \varepsilon z(s))$. Second, we have

$$\Delta_\Sigma X = 2HN,$$

where Δ_Σ is the Laplace-Beltrami operator on Σ and N is a unit normal on Σ (cf. [6], pp.72–74). As a result, problem (2.28) reduces the the following problem for $r(s)$ and $z(s)$ (cf. [1], p.463):

$$\begin{aligned} &r'' = -\frac{\varepsilon^2\lambda z'}{(1+z)^2} + \frac{\varepsilon^2 (z')^2}{r}, \qquad z'' + \frac{r'z'}{r} = \frac{\lambda r'}{(1+z)^2}, \qquad 0 < s < \ell; \\ &r(0) = 0, \ r'(0) = 1, \ r(\ell) = 1, \ z'(0) = 0, \ z(\ell) = 0, \end{aligned} \tag{2.29}$$

where λ and ℓ are unknown parameters to be determined. Furthermore, to facilitate the analysis of the upper solution branch, we impose the condition $z(0) = -1 + \delta$ and study problem (2.29) in the limits $\varepsilon \to 0^+$ and $\delta \to 0^+$, where the relationship between these two small parameters is to be determined. In the outer region away from $s = 0$, we

expand r, z, λ and ℓ as

$$\begin{aligned} r(s;\varepsilon) &= r_0(s) + \varepsilon^2 r_1(s) + \varepsilon^4 r_2(s) + \mathcal{O}(\varepsilon^6), \\ z(s;\varepsilon) &= z_0(s) + \varepsilon^2 z_1(s) + \varepsilon^4 z_2(s) + \mathcal{O}(\varepsilon^6), \end{aligned} \tag{2.30 a}$$

and

$$\lambda(\varepsilon) = \lambda_0 + \varepsilon^2\lambda_1 + \varepsilon^4\lambda_2 + \mathcal{O}(\varepsilon^6), \qquad \ell(\varepsilon) = \ell_0 + \varepsilon^2\ell_1 + \varepsilon^4\ell_2 + \mathcal{O}(\varepsilon^6), \tag{2.30 b}$$

which upon substituting into problem (2.29) gives

$$\begin{aligned} &r_0'' = 0, \qquad z_0'' + \frac{r_0' z_0'}{r_0} = \frac{\lambda_0 r_0'}{(1+z_0)^2}, \qquad 0 < s < 1; \\ &r_0(0) = 0,\ r_0'(0) = 1,\ r_0(\ell_0) = 1,\ z(0) = -1,\ z_0'(0) = 0,\ z_0(\ell_0) = 0, \end{aligned} \tag{2.31}$$

at order $\mathcal{O}(1)$. Therefore in solving problem (2.31) we find

$$r_0(s) = s, \quad z_0(s) = -1 + s^{2/3}, \quad \lambda_0 = \frac{4}{9}, \quad \ell_0 = 1. \tag{2.32}$$

However, $z_0'(0) \neq 0$ and therefore, we have a boundary layer at $s = 0$ for $z(s)$. Next, from (2.29), (2.30) and (2.32) we have

$$\begin{aligned} &r_1'' = \frac{4}{27}s^{-5/3}, \qquad z_1'' + \frac{1}{s}z_1' + \frac{8}{9s^2}z_1 = \frac{2}{3}\frac{r_1}{s^{7/3}} + \frac{9\lambda_1 - 2r_1'}{9s^{4/3}}, \\ &r_1(0) = 0,\ r_1'(0) = 0,\ r_1(1) = -\ell_1,\ z_1(1) = -\frac{2}{3}\ell_1, \end{aligned} \tag{2.33}$$

at order $\mathcal{O}(\varepsilon^2)$. The solution for $r_1(s)$ is

$$r_1(s) = \left(\frac{2}{3} - \ell_1\right)s - \frac{2}{3}s^{1/3} \tag{2.34}$$

where the condition $r_1'(0) = 0$ will be enforced in the boundary layer at $s = 0$. Then using solution (2.34) in problem (2.33), we obtain

$$z_1'' + \frac{1}{s}z_1' + \frac{8}{9s^2}z_1 = -\frac{32}{81s^2} + \left(\lambda_1 + \frac{8}{27} - \frac{4}{9}\ell_1\right)\frac{1}{s^{4/3}}, \qquad z_1(1) = 0,$$

which upon solving gives

$$z_1(s) = \frac{(27\lambda_1 + 8 - 12\ell_1)}{36}s^{2/3} - \frac{4}{9} + A_1\sin\left(\omega\log s + \phi_1\right), \quad \omega := \frac{2\sqrt{2}}{3}. \tag{2.35}$$

Here, A_1 and φ_1 are constants that will be determined by matching and the value of λ_1 will be determined later by applying the condition $z_1(1) = -2\ell_1/3$. In order to fix the value of ℓ_1, an expansion to higher order is required. Accordingly, we use (2.30) in (2.29) to find a system of differential equations at order $\mathcal{O}(\varepsilon^4)$ (see Appendix B), which upon solving gives

$$r_2(s) = \frac{K_1}{s^{1/3}} + K_2 + \frac{6\ell_1 - 4 + 36A_1\sin\phi_1}{27}s^{1/3} + C_2 s,$$

where

$$\begin{aligned} K_1 &:= \frac{2 + 4\sqrt{2}A_1\cos\left(\omega\log s + \phi_1\right) - 16A_1\sin\left(\omega\log s + \phi_1\right)}{27}, \\ K_2 &:= \left(\frac{2}{27} - \frac{2\ell_1}{3} + {\ell_1}^2 - \ell_2 - C_2 - \frac{2}{9}\omega A_1\cos\phi_1 - \frac{20}{27}A_1\sin\phi_1\right), \end{aligned}$$

and

$$z_2(s) = \frac{K_3}{s^{2/3}} + \frac{K_4}{s^{1/3}} + \frac{4}{3}A_1 \sin\phi_1 + A_2 \sin\left(\omega \log s + \phi_2\right) + K_5 s^{2/3},$$

where

$$\begin{aligned} K_3 :=& \frac{2}{81} + \frac{{A_1}^2}{2} - \frac{58\sqrt{2}}{81}A_1 \cos\left(\omega \log s + \phi_1\right) - \frac{20}{81}A_1 \sin\left(\omega \log s + \phi_1\right) \\ &+ \frac{5}{38}{A_1}^2 \cos\left(2\omega \log s + 2\phi_1\right) + \frac{2\sqrt{2}}{19}{A_1}^2 \sin\left(2\omega \log s + 2\phi_1\right), \end{aligned}$$

$$\begin{aligned} K_4 :=& \frac{4 - 36\ell_1 + 54{\ell_1}^2 - 54\ell_2 - 54C_2 - 8\sqrt{2}A_1 \cos\phi_1 - 40A_1 \sin\phi_1}{18}, \\ K_5 :=& \frac{48\ell_1 - 36{\ell_1}^2 - 16 - 162{A_1}^2 + 243\lambda_2 + 108C_2}{324} \\ &+ \frac{9{A_1}^2 \cos 2\phi_1 - 2A_1(3\ell_1 - 2)\sin\phi_1}{18}. \end{aligned}$$

Next we introduce the inner variable $\rho = s/\gamma$, which after plugging into z_0 gives the near field behavior $z = -1 + \gamma^{2/3}\rho + \cdots$ as $s \to 0^+$. Moreover, $z = -1 + \mathcal{O}(\delta)$ in the inner layer, and as a result, we choose $\gamma = \delta^{3/2}$. Then for matching we write the outer solution, (2.30 *a*), in terms of the inner variable, $\rho = s/\delta^{3/2}$, to obtain

$$\begin{aligned} r =& \delta^{3/2}\left(\rho - \frac{2\delta_0}{3}\rho^{1/3} + \frac{{\delta_0}^2 K_1}{\rho^{1/3}}\right) + \delta^2 {\delta_0}^2 K_2 \\ &+ \delta^{5/2}\left(\delta_0\left(\frac{2}{3} - \ell_1\right)\rho + \frac{{\delta_0}^2(6\ell_1 - 4 + 36A_1 \sin\phi_1)}{27}\rho^{1/3}\right) + \mathcal{O}(\delta^{7/2}) \end{aligned} \tag{2.36 a}$$

and

$$\begin{aligned} z =& -1 + \delta\left(\rho^{2/3} - \frac{4\delta_0}{9} + \delta_0 A_1 \sin\left(\omega \log\rho + \sqrt{2}\log\delta + \phi_1\right) + \frac{{\delta_0}^2 K_3}{\rho^{2/3}}\right) \\ &+ \delta^{3/2}\frac{{\delta_0}^2 K_4}{\rho^{1/3}} \\ &+ \delta^2\left(\left(\frac{(4 - 6\ell_1)\delta_0}{9} - \delta_0 A_1 \sin\phi_1\right)\rho^{2/3}\right. \\ &\left. + \frac{4{\delta_0}^2}{3}A_1 \sin\phi_1 + {\delta_0}^2 A_2 \sin\left(\omega \log\left(\delta^{3/2}\rho\right) + \phi_2\right)\right) + \mathcal{O}(\delta^3) \end{aligned} \tag{2.36 b}$$

as $s \to 0^+$. It will be seen that the inner solution cannot be matched to the order $\mathcal{O}(\delta^2)$ of expansion (2.36 *a*). For this reason, the constant C_2 is chosen such that K_2 vanishes, which causes K_4 to vanish and gives the reduced local behavior

$$\begin{aligned} r =& \delta^{3/2}\left[\rho - \frac{2\delta_0}{3}\rho^{1/3} + \mathcal{O}(\rho^{-1/3})\right. \\ &\left. + \delta\left(\delta_0\left(\frac{2}{3} - \ell_1\right)\rho + \frac{{\delta_0}^2(6\ell_1 - 4 + 36A_1 \sin\phi_1)}{27}\rho^{1/3}\right) + \mathcal{O}(\delta^2)\right], \end{aligned} \tag{2.37 a}$$

and

$$z = -1 + \delta\left[\rho^{2/3} - \frac{4\delta_0}{9} + \delta_0 A_1 \sin\left(\omega\log\rho + \sqrt{2}\log\delta + \varphi_1\right) + \mathcal{O}(\rho^{-2/3}) \right. \\ \left. + \delta\left(\left(\frac{(4-6\ell_1)\delta_0}{9} - \delta_0 A_1 \sin\phi_1\right)\rho^{2/3} + \mathcal{O}(1)\right) + \mathcal{O}(\delta^2)\right], \tag{2.37 b}$$

as $s \to 0^+$. As a consequence, these local expansions motivate us to introduce the following local variables within the vicinity of $s = 0$:

$$\rho = s/\delta^{3/2}, \quad r(s) = \delta^{3/2} R(\rho), \qquad z(s) = -1 + \delta Z(\rho). \tag{2.38}$$

These new variables then transform the system of differential equations in (2.29) into

$$R'' = \frac{\varepsilon^2}{\delta}\left(-\frac{\lambda Z'}{Z^2} + \frac{(Z')^2}{R}\right), \qquad Z'' + \frac{R'Z'}{R} = \frac{\lambda R'}{Z^2}. \tag{2.39}$$

Here a dominant balances requires $\varepsilon^2/\delta = \delta_0$, where $\delta_0 = \mathcal{O}(1)$. Therefore, expanding R and Z as

$$R = R_0 + \delta R_1 + \mathcal{O}(\delta^2), \quad Z = Z_0 + \delta Z_1 + \mathcal{O}(\delta^2), \tag{2.40}$$

respectively, we find that the leading order problem for the inner solution is

$$\begin{aligned} &R_0'' = -\delta_0\frac{\lambda_0 Z_0'}{Z_0^2} + \delta_0\frac{(Z_0')^2}{R_0}, \qquad Z_0'' + \frac{R_0' Z_0'}{R_0} = \frac{\lambda_0 R_0'}{Z_0^2}, \qquad 0 < \rho < \infty; \\ &R_0(0) = 0,\ R_0'(0) = 1,\ Z_0(0) = 1,\ Z_0'(0) = 0. \end{aligned} \tag{2.41}$$

To find the far field behavior of R_0 and Z_0, we assume $R_0 \sim \rho + V$ as $\rho \to \infty$, where $V \ll \rho$, and $Z_0 \sim \rho^{2/3} + W$ as $\rho \to \infty$, where $W \ll \rho^{2/3}$. Substituting these relations into problem (2.41), gives asymptotic differential equations for $V(\rho)$ and $W(\rho)$,

$$V'' \sim \frac{4\delta_0}{27}\rho^{-5/3}, \quad W'' + \frac{W'}{\rho} + \frac{2\lambda_0}{\rho^2}W \sim -\frac{32\delta_0}{81}\frac{1}{\rho^2}, \qquad \text{as } \rho \to \infty,$$

whose solution is $V \sim -(2\delta_0/3)\rho^{1/3}$, $W \sim -\delta_0\lambda_0 + \tilde{A}_1(\delta_0)\sin(\omega\log\rho + \tilde{\phi}_1(\delta_0))$ as $\rho \to \infty$. Hence, the far field behavior for the solution, R_0 and Z_0 of problem (2.41) is

$$\begin{aligned} &R_0(\rho) = \rho - \frac{2\delta_0}{3}\rho^{1/3} + \mathcal{O}(1), \\ &Z_0(\rho) = \rho^{2/3} - \delta_0\lambda_0 + \tilde{A}_1(\delta_0)\sin\left(\omega\log\rho + \tilde{\phi}_1(\delta_0)\right) + \mathcal{O}(1), \end{aligned} \qquad \text{as } \rho \to \infty. \tag{2.42}$$

Proceeding to $\mathcal{O}(\delta)$ terms, we substitute the expansions in (2.40) into problem (2.39) to find that R_1 and Z_1 satisfy

$$\begin{aligned} &R_1'' = \delta_0\left(-\frac{\delta_0\lambda_1 Z_0' + \lambda_0 Z_1}{Z_0^2} + \frac{2\lambda_0 Z_1 Z_0'}{Z_0^3} - \frac{R_1 Z_0'^2}{R_0^2} + \frac{2Z_0' Z_1'}{R_0}\right),\ 0 < \rho < \infty, \\ &Z_1'' = \frac{\delta_0\lambda_1 R_0' + \lambda_0 R_1'}{Z_0^2} - \frac{2\lambda_0 Z_1 R_0'}{Z_0^3} + \frac{R_1 R_0' Z_0'}{R_0^2} - \frac{R_1' Z_0' + R_0' Z_1'}{R_0},\ 0 < \rho < \infty, \\ &R_1(0) = 0,\ R_1'(0) = 0,\ Z_1(0) = 0,\ Z_1'(0) = 0. \end{aligned} \tag{2.43}$$

From the expansions in (2.37) we expect the far field behavior of both R_1 and Z_1 to grow algebraically. Therefore, we assume $R_1 \sim a\rho^\alpha$ and $Z_1 \sim b\rho^\beta$ as $\rho \to \infty$ and substitute

this behavior into problem (2.43) along with the far field behavior of R_0 and Z_0. After a dominant balance, this yields

$$a\alpha(\alpha-1)\rho^{\alpha-2} \sim -\frac{2{\delta_0}^2\lambda_1}{3}\rho^{-5/3} + \left(\frac{4b\beta\delta_0}{3} + \frac{4b\delta_0\lambda_0}{3} - b\beta\delta_0\lambda_0\right)\rho^{\beta-7/3},$$
$$b\beta(\beta-1)\rho^{\beta-2} \sim \delta_0\lambda_1\rho^{-4/3} - b\left(\beta+2\lambda_0\right)\rho^{\beta-2},$$

as $\rho \to \infty$. Consequently,

$$a = -{\delta_0}^2\lambda_1, \quad \alpha = \frac{1}{3}, \quad b = \frac{3\delta_0\lambda_1}{4}, \quad \beta = \frac{2}{3},$$

which implies that

$$R_1 \sim -{\delta_0}^2\lambda_1\rho^{1/3}, \qquad Z_1 \sim \frac{3\delta_0\lambda_1}{4}\rho^{2/3}, \quad \text{as } \rho\to\infty. \tag{2.44}$$

As a result, expansions (2.40), (2.42) and (2.44) give the following far field behavior of the inner solution:

$$\begin{aligned} R &= \left(\rho - \frac{2\delta_0}{3}\rho^{1/3} + \cdots\right) + \delta\left(-{\delta_0}^2\lambda_1\rho^{1/3} + \cdots\right) + \mathcal{O}(\delta^2), \\ Z &= \left(\rho^{2/3} - \delta_0\lambda_0 + \tilde{A}_1(\delta_0)\sin\left(\omega\log\rho + \tilde{\phi}_1(\delta_0)\right) + \cdots\right) \\ &\quad + \delta\left(\frac{3\delta_0\lambda_1}{4}\rho^{2/3} + \cdots\right) + \mathcal{O}(\delta^2) \end{aligned} \tag{2.45}$$

as $\delta \to 0^+$ and $\rho \to \infty$. Then for matching we compare (2.38), using (2.45), with (2.37) to get

$$\ell_1 = \frac{2}{3}, \quad A_1 = \frac{\tilde{A}_1(\delta_0)}{\delta_0}, \quad \phi_1 = \tilde{\phi}_1(\delta_0) - \sqrt{2}\log\delta, \quad \lambda_1 = -\frac{4}{3}A_1\sin\phi_1. \tag{2.46}$$

Note that the boundary condition $z_1(1) = -2\ell_1/3$ is automatically satisfied by the value of λ_1 determined in (2.46). By returning to the definition of λ made in (2.30 *b*) and recalling that $\varepsilon^2/\delta = \delta_0$, a two term expansion of λ is now given by

$$\lambda = \frac{4}{9} - \delta\,\frac{4}{3}\,\tilde{A}_1(\varepsilon^2/\delta)\sin\left[-\sqrt{2}\log\delta + \tilde{\phi}_1(\varepsilon^2/\delta)\right] + \cdots.$$

Next, we fix ε in governing problem (2.29). Therefore, for our asymptotic analysis to remain valid, we need $\varepsilon^2/\delta = \delta_0 = \mathcal{O}(1)$, leading to the following asymptotic result regarding the upper solution branch of the bifurcation diagram of (2.29).

Principal Result 2.3 *For solutions of* (1.4) *with* $\partial\Omega = \partial B_1(0)$*, there is a regime where both* $\varepsilon \ll 1$ *and* $\delta \ll 1$*, with* $\varepsilon^2/\delta = \mathcal{O}(1)$*, such that the upper solution branch of the bifurcation curve has the asymptotic parameterization,* $(\lambda(\delta;\varepsilon), |z(0)|)$*, where*

$$|z(0)| = 1-\delta, \qquad \lambda = \lambda_0 - \delta\,\frac{4}{3}\,\tilde{A}_1(\varepsilon^2/\delta)\sin\left[-\sqrt{2}\log\delta + \tilde{\phi}_1(\varepsilon^2/\delta)\right] + \mathcal{O}(\delta^2). \tag{2.47}$$

Moreover, $\lambda_0 = 4/9$*, and* $\tilde{A}_1(\delta_0)$ *and* $\tilde{\phi}_1(\delta_0)$ *are functions determined by the far field behavior of* Z_0*,*

$$Z_0(\rho) = \rho^{2/3} - \frac{4\delta_0}{9} + \tilde{A}_1(\delta_0)\sin\left(\omega\log\rho + \tilde{\phi}_1(\delta_0)\right) + o(1) \quad \text{as } \rho\to\infty, \tag{2.48 a}$$

of the initial value problem

$$\begin{aligned} &R_0'' = -\frac{4\delta_0}{9}\frac{Z_0'}{{Z_0}^2} + \delta_0\frac{(Z_0')^2}{R_0}, \qquad Z_0'' + \frac{R_0'Z_0'}{R_0} = \frac{4}{9}\frac{R_0'}{{Z_0}^2}, \qquad 0<\rho<\infty; \\ &R_0(0)=0,\ R_0'(0)=1,\ Z_0(0)=1,\ Z_0'(0)=0, \end{aligned} \tag{2.48 b}$$

where

$$R_0(\rho) = \rho - \frac{2\delta_0}{3}\rho^{1/3} + \mathcal{O}(1) \quad \textit{as } \rho\to\infty. \tag{2.48 c}$$

To study the accuracy of this result, we compute the functions $\tilde{A}_1(\delta_0)$ and $\tilde{\phi}_1(\delta_0)$ as in §2.2 (see Figure 10). As expected, these new functions are continuations of those found in Principal Result 2.1.

A combination of the asymptotic formula (2.47) and the numerically obtained functions $\tilde{A}_1(\delta_0)$ and $\tilde{\phi}_1(\delta_0)$ allow for a reconstruction of the bifurcation diagram (see Figure 11).

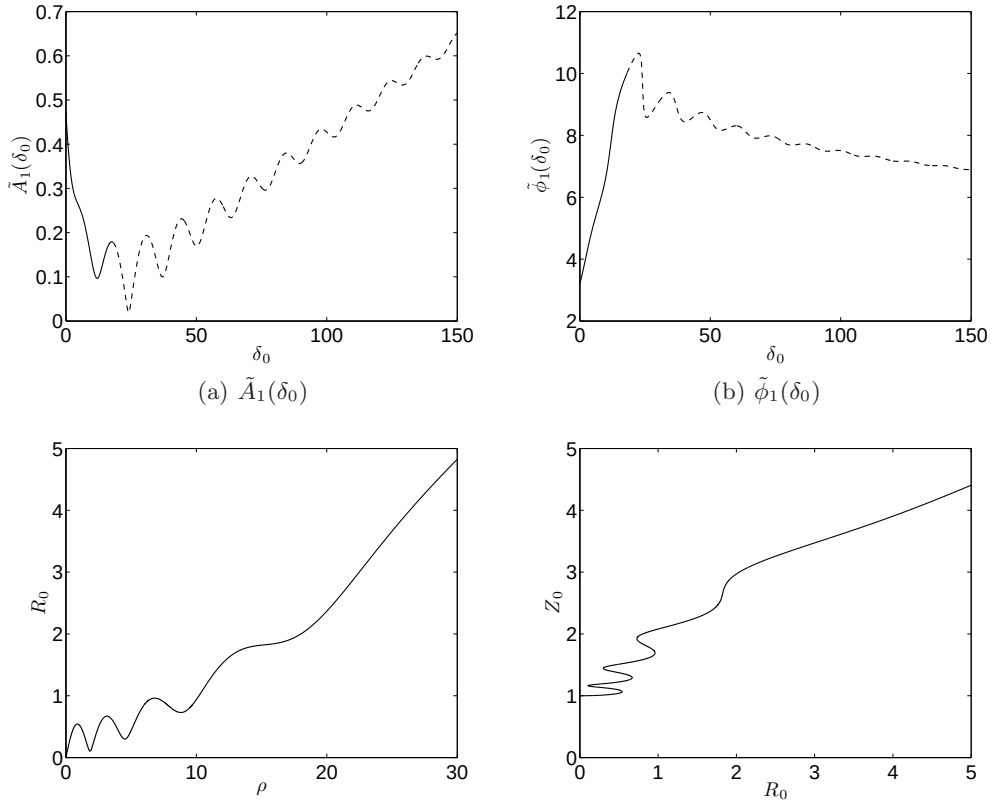

(a) $\tilde{A}_1(\delta_0)$ (b) $\tilde{\phi}_1(\delta_0)$

(c) $R_0(\rho)$, $\delta_0 = 75$. (d) R_0 vs Z_0, $\delta_0 = 75$.

FIGURE 10. Upper left and right: Graphs of $\tilde{A}_1(\delta_0)$ and $\tilde{\phi}_1(\delta_0)$ against δ_0 computed from (2.48). The solid line indicates where the coefficients agree with those computed from (2.19 *a*). Lower left and right: Plots of $R_0(\rho)$ vs ρ and $R_0(\rho)$ vs $Z_0(\rho)$ for $\delta_0 = 75$. The oscillatory nature of R_0 observed in (c) accounts for the multivalued solutions shown in (d).

Numerically, $\tilde{A}_1(\delta_0)$ appears to grow linearly as $\delta_0 \to \infty$, which would indicate that $\delta\tilde{A}_1(\varepsilon^2/\delta)$ is finite as $\delta \to 0$. Therefore the analysis predicts that the upper solution branch of problem (2.29) undergoes infinitely many fold points in a way similar to the upper branch of problem (1.3) for the two-dimensional unit disk. This prompts the following conjecture.

Conjecture 2.8 *For $\varepsilon > 0$ fixed and sufficiently small, the upper solution branch of the bifurcation diagram of problem* (1.4)*, with $\partial\Omega$ equal to the unit circle, undergoes infinitely many folds. Also as $|z(0)| \to 1^-$, the nonlinear eigenvalue $\lambda > 0$ goes to a finite value that is bounded away from zero.*

In Figure 11, asymptotic approximation (2.47) is compared with the numerically computed bifurcation diagram of problem (2.28). From this we see that the observed agreement is very good.

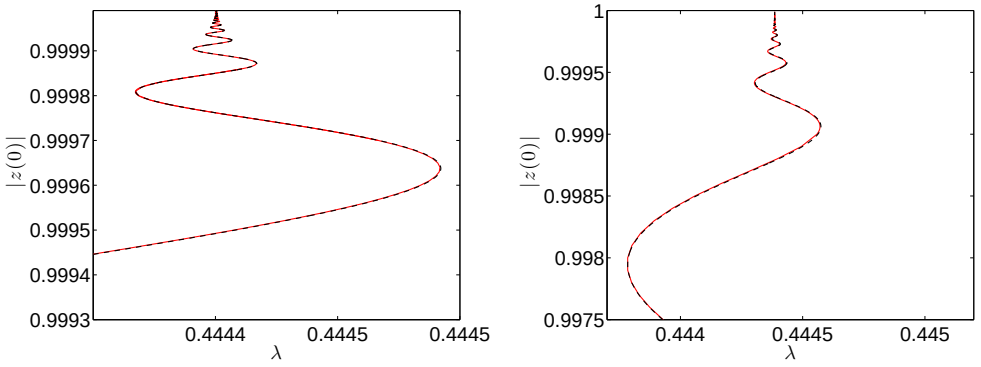

(a) $\varepsilon = 0.05$ (b) $\varepsilon = 0.1$

FIGURE 11. Comparison of the full numerical solution of the bifurcation curve for (1.1) in $B_1(0)$ (solid) with asymptotic formula (2.18) (dashed) for: (a) $\varepsilon = 0.05$; (b) $\varepsilon = 0.1$. In both (a) and (b), the asymptotic prediction agrees extremely well with the full numerical solution.

3 Conclusion

In this work, we have analyzed the *upper branch* of solutions to problem (2.28) in the limit $\|u\|_\infty \to 1^-$. In this situation there are marked differences between the solution structure for $\varepsilon = 0$ and $\varepsilon > 0$. We have shown that for any $\varepsilon > 0$, solutions u of problem (1.1) in $B_1(0)$ do not exist for $\|u\|_\infty$ arbitrarily close to 1. Also, it is observed that as the upper solution branch is traversed, a singularity in the first derivative of the solution develops in the interior of the domain, and at this singularity, the branch of solutions ends abruptly at a single dead-end point. Our asymptotic analysis allows for an accurate prediction of this point to be made by relating it to a singularity in an associated initial value problem. Moreover, our analysis predicts that the singularity occurs for a fixed value of $\varepsilon^2/(1+\|u\|_\infty)$ and therefore establishes a relationship between a given ε and the

dead-end point. In each case, the asymptotic parameterizations obtained for the solution branch compare very well with full numerical solutions.

Finally, by studying a parametric version of problem (1.1), we find and analyze a new family of solutions emanating from the dead-end point. These solutions are found to be strictly parametric and provide a natural continuation of the bifurcation curve beyond the dead-end point. This new solution branch retains the infinite fold points feature of the $\varepsilon = 0$ problem.

The main limitation of our study is that we deal only with the two-dimensional unit ball domain. Though our analysis has revealed interesting structure, an investigation of problem (1.1) in more general domains would be desirable; specifically, can a result like Theorem 2.3 be formulated. Additionally, it would be interesting to study solutions of problem (1.1) in the unit ball in higher spatial dimensions. It has been rigorously established that when $B_1(0) \subset \mathbb{R}^n$ and $2 \leqslant n \leqslant 7$, the bifurcation diagram of problem (1.3) exhibits the infinite fold points structure [11]. What then is the effect of positive ε on the bifurcation structure of (1.1) when $n \geqslant 3$?

Another interesting avenue for future investigation is the dynamic version of problem (1.1), namely the equation

$$\begin{aligned} u_t = \operatorname{div} \frac{\nabla u}{\sqrt{1+\varepsilon^2|\nabla u|^2}} - \frac{\lambda}{(1+u)^2} \quad \text{in } \Omega \times (0,T); \\ u(x,0) = 0 \quad \text{in } \Omega, \qquad u = 0 \quad \text{in } \partial\Omega \times (0,T). \end{aligned} \tag{3.1}$$

Is there an equivalent of disappearance of solutions for problem (3.1), *i.e.*, does u or its derivatives exhibit a singularity at some finite t before reaching $u = -1$?

Acknowelegments

The first author (N.D.B.) thanks the National Science Foundation for their support through the Graduate Research Fellowship Program. Also, N.D.B. would like to thank J. A. Pelesko for many useful discussions. A.E.L acknowledges financial support from the Carnegie Trust for the Universities of Scotland and the Centre for Analysis and Nonlinear PDEs (UK EPSRC Grant EP/E03635X).

Appendix A

To solve (2.29) numerically, we use a shooting method. That is, we impose the initial conditions

$$r(0) = 0, \; r'(0) = \ell, \; z'(0) = 0, \; z(0) = \alpha, \tag{A 1}$$

where $\alpha \in (-1, 0)$ and find (λ, ℓ) such that $F(\lambda, \ell) := \begin{bmatrix} r(1;\lambda,\ell) - 1 & z(1;\lambda,\ell) \end{bmatrix}^T = \mathbf{0}$. To do so, we apply Newton's method and iterate as

$$\boldsymbol{\lambda}_{n+1} = \boldsymbol{\lambda}_n - \begin{bmatrix} \dfrac{\partial r}{\partial \lambda}(1;\lambda_n,\ell_n) & \dfrac{\partial r}{\partial \ell}(1;\lambda_n,\ell_n) \\ \dfrac{\partial z}{\partial \lambda}(1;\lambda_n,\ell_n) & \dfrac{\partial z}{\partial \ell}(1;\lambda_n,\ell_n) \end{bmatrix}^{-1} \begin{bmatrix} r(1;\lambda_n,\ell_n) - 1 \\ (1;\lambda_n,\ell_n) \end{bmatrix}$$

where $\boldsymbol{\lambda}_n = \begin{bmatrix}\lambda_n & \ell_n\end{bmatrix}^T$. Therefore at each step we need to find $r_\lambda(1;\lambda_n,\ell_n)$, $r_\ell(1;\lambda_n,\ell_n)$, $z_\lambda(1;\lambda_n,\ell_n)$ and $z_\ell(1;\lambda_n,\ell_n)$. To this end, we differentiate the ode given in (2.29) and the initial conditions (A 1) with respect to λ and separately with respect to ℓ to get two auxiliary problem for (r_λ, z_λ) and (r_ℓ, z_ℓ), whose solutions evaluated at $\xi = 1$ yield our desired result.

Appendix B

Here are the order $\mathcal{O}(\varepsilon^4)$ outer ODEs for (2.29):

$$\begin{aligned}
&r_2'' = \frac{M_1}{s^{7/3}} + \frac{M_2}{s^{5/3}},\\
&r_2(1) = \ell_1(\ell_1 - \lambda_0) - \ell_2,\\
&z_2'' + \frac{1}{s}z_2' + \frac{2\lambda_0}{s^2}z_2 = \frac{2r_2}{3s^{7/3}} - \frac{2r_2'}{9s^{4/3}} - \frac{M_3}{s^2} + \frac{M_4}{s^{4/3}} - \frac{M_5}{s^{8/3}}\\
&z_2(1) = \frac{\ell_1(15\ell_1 - 8)}{27} - \frac{2\ell_2}{3} + \frac{2A_1\ell_1}{3}(\sin\phi_1 - \sqrt{2}\cos\phi_1)
\end{aligned} \tag{B 1}$$

where

$$\begin{aligned}
M_1 &:= \frac{144\sqrt{2}A_1\cos\left(\frac{2\sqrt{2}}{3}\log s + \phi_1\right) + 144A_1\sin\left(\frac{2\sqrt{2}}{3}\log s + \phi_1\right) + 8}{243}\\
M_2 &:= \frac{8 - 12\ell_1 - 72A_1\sin\phi_1}{243}\\
M_3 &:= \frac{32(3 - 2\ell_1 - 9A_1\sin\phi_1)}{729}\\
M_4 &:= \frac{227 + 48\ell_1 - 36{\ell_1}^2 - 36A_1(3\ell_1 - 2)\sin\phi_1 - 324{A_1}^2\sin^2\phi_1}{243}\\
M_5 &:= \frac{4\left(4 + 54\sqrt{2}A_1\cos\left(\frac{2\sqrt{2}}{3}\log s + \phi_1\right) + 180A_1\sin\left(\frac{2\sqrt{2}}{3}\log s + \phi_1\right)\right)}{729}\\
&\quad - \frac{4{A_1}^2\sin^2\left(\frac{2\sqrt{2}}{3}\log s + \phi_1\right)}{3}
\end{aligned}$$

and we have simplified the result using (2.32), (2.34), (2.35) and (2.46).

References

[1] N. D. Brubaker and J. A. Pelesko, *Non-linear effects on canonical MEMS models*, European J. Appl. Math., 22 (2011), pp. 455–470.

[2] ———, *Analysis of a one-dimensional prescribed mean curvature equation with singular nonlinearity*, Nonlinear Anal., 75 (2012), pp. 5086–5102.

[3] M. Burns and M. Grinfeld, *Steady state solutions of a bi-stable quasi-linear equation with saturating flux*, European J. Appl. Math., 22 (2011), pp. 317–331.

[4] P. Concus and R. Finn, *The shape of a pendent liquid drop*, Philos. Trans. Roy. Soc. London Ser. A, 292 (1979), pp. 307–340.

[5] P. Coullet, L. Mahadevan, and C. S. Riera, *Hydrodynamical models for the chaotic dripping faucet*, J. Fluid Mech., 526 (2005), pp. 1–17.

[6] U. Dierkes, S. Hildebrandt, and F. Sauvigny, *Minimal Surfaces*, vol. 339 of

Grundlehren der mathematischen Wissenschaften, Springer-Verlag, Heidelberg, 2nd ed., 2010.

[7] P. Esposito, N. Ghoussoub, and Y. Guo, *Mathematical Analysis of Partial Differential Equations Modeling Electrostatic MEMS*, vol. 20 of Courant Lecture Notes in Mathematics, AMS/CIMS, New York, 2010.

[8] R. Finn, *Equilibrium Capillary Surfaces*, no. 284 in Grundlehren der mathematischen Wissenschaften, Springer-Verlag, New York, 1986.

[9] D. Gilbarg and N. S. Trudinger, *Elliptic Partial Differential Equations of Second Order*, no. 224 in Grundlehren der mathematischen Wissenschaften, Springer-Verlag, Berlin, 2nd ed., 1983.

[10] Y. Guo, Z. Pan, and M. J. Ward, *Touchdown and pull-in voltage behavior of a MEMS device with varying dielectric properties*, SIAM J. Appl. Math., 66 (2005), pp. 309–338.

[11] Z. Guo and J. Wei, *Infinitely many turning points for an elliptic problem with a singular non-linearity*, J. Lond. Math. Soc. (2), 78 (2008), pp. 21–35.

[12] V. K. Le, *On a sub-supersolution method for the prescribed mean curvature problem*, Czechoslovak Math. J., 58 (2008), pp. 541–560.

[13] A. E. Lindsay and M. J. Ward, *Asymptotics of some nonlinear eigenvalue problems for a MEMS capacitor. Part I: Fold point asymptotics*, Methods Appl. Anal., 15 (2008), pp. 297–326.

[14] ———, *Asymptotics of some nonlinear eigenvalue problems modelling a MEMS capacitor. Part II: Multiple solutions and singular asymptotics*, European J. Appl. Math., 22 (2011), pp. 83–123.

[15] D. E. Moulton and J. A. Pelesko, *Theory and experiment for soap-film bridge in an electric field*, J. Colloid Interface Sci., 322 (2008), pp. 252–262.

[16] H. Pan, *One-dimensional prescribed mean curvature equation with exponential nonlinearity*, Nonlinear Anal., 70 (2009), pp. 999–1010.

[17] H. Pan and R. Xing, *Time maps and exact multiplicity results for one-dimensional prescribed mean curvature equations*, Nonlinear Anal., 74 (2011), pp. 1234–1260.

[18] ———, *Time maps and exact multiplicity results for one-dimensional prescribed mean curvature equations. II*, Nonlinear Anal., 74 (2011), pp. 3751–3768.

[19] ———, *Radial solutions for a prescribed mean curvature equation with exponential nonlinearity*, Nonlinear Anal., 75 (2012), pp. 103–116.

[20] J. A. Pelesko and D. H. Bernstein, *Modeling MEMS and NEMS*, Chapman & Hall/CRC, Boca Raton, FL, 2003.

[21] M. H. Protter and H. F. Weinberger, *Maximum Principles in Differential Equations*, Springer, New York, 1967.

[22] P. Pucci and J. Serrin, *The Maximum Principle*, no. 73 in Progess in Nonlinear Differential Equations and Their Applications, Birkhauser, Basel, 2007.

[23] H. C. Wente, *The symmetry of sessile and pendent drops*, Pacific J. Math., 88 (1980), pp. 387–397.